Effects of Hydraulic Loading History on Suffusion Susceptibility of Cohesionless Soils

Abdul Rochim, Ph.D.[1]; Didier Marot[2]; Luc Sibille, Ph.D.[3]; and Van Thao Le[4]

Abstract: Suffusion is a selective erosion of fine particles under the effect of seepage flow within the matrix of coarser particles. This complex phenomenon appears as a combination of three processes: detachment, transport, and possible filtration of finer fraction. It can induce a change in particle size distribution, porosity, and hydraulic conductivity of the material. With the objective to characterize suffusion susceptibility, downward seepage flow tests were conducted. Four different cohesionless soils were tested under hydraulic-gradient controlled conditions or under flow-rate controlled conditions. This study shows the significant effect of hydraulic loading history on the value of critical hydraulic gradient. Moreover, the method characterizing the erosion susceptibility based on rate of erosion does not lead to a unique characterization of suffusion process for different types of hydraulic loading. The new analysis is based on energy expended by the seepage flow and the cumulative eroded dry mass. The results demonstrate that this approach is more effective to characterize suffusion susceptibility for cohesionless soils. **DOI: 10.1061/(ASCE)GT.1943-5606.0001673.** © *2017 American Society of Civil Engineers.*

Introduction

Hydraulic earth structures can suffer from instabilities induced by internal erosion processes. Fry et al. (2012) indicated that overtopping and internal erosion are the two main causes of failure of embankment dams and dikes.

Fell and Fry (2013) distinguished four forms of internal erosion: concentrated leak erosion, backward erosion, contact erosion, and suffusion. This paper deals with suffusion, which can induce a change in particle size distribution, porosity, and hydraulic conductivity of the soil. Moreover, although the suffusion development may be difficult to detect in situ, it has to be considered with attention as it can evolve toward a second phase of erosion, characterized by a blowout and an extensive erosion of fine particles, inducing both a large settlement of the specimen and a relatively strong increase in the hydraulic conductivity (Sibille et al. 2015b). Thus to ensure the safety assessment of hydraulic earth structures, the characterization of suffusion susceptibility is required. Nevertheless, only recently was a method for classifying the suffusion

susceptibility of soils based on experimental results proposed (Marot et al. 2016).

Soils that are likely to suffer from suffusion have a grain-size distribution curve either discontinuous or upwardly concave (Fell and Fry 2007), and even with a slight variation of the initial gradation, an abrupt transition appears between internally stable and unstable states (Skempton and Brogan 1994).

In comparison with the time scale in a laboratory, in situ the hydraulic loading can be applied on soils, constituting the hydraulic earth structures and its foundations, over a very long timespan. The upstream head applied on an earth structure can increase by several cm per hour in case of flood, rapid reservoir filling, or heavy rain seasons, but only a few mm per day under normal flow conditions. The corresponding values of increment of hydraulic gradient depend on the earth structure's design and also on the studied position in this structure. Moreover the seepage flow depends on not only the aforementioned parameters but also on hydraulic conductivity of soils. Thus to optimize the test duration and to take into account this large range of possible hydraulic loadings, researchers performed internal erosion tests under various hydraulic loading conditions. Suffusion tests described in literature were mostly performed under multistaged hydraulic gradient conditions in upward direction with hydraulic gradients ranging from 0.02 to 1.4 (Skempton and Brogan 1994; Ke and Takahashi 2012; Indraratna et al. 2015) or in downward direction with the hydraulic gradient range from 0.15 to 9.4 (Moffat and Fannin 2006; Chang and Zhang 2011). But other tests were also done under single-staged hydraulic gradients with values between 5 and 140 (Bendahmane et al. 2008; Wan and Fell 2008; Nguyen et al. 2012). Nguyen et al. (2012) and Ke and Takahashi (2014, 2015) performed suffusion tests under flow-rate controlled conditions with a range of discharge per unit cross section from 10^{-3} to 0.13 cm · s^{-1}. Kenney and Lau (1985) described their test conditions as severe because the values of discharge per unit cross section were larger than those usually encountered in engineering practice with similarly graded materials (0.37–1.67 cm · s^{-1}). However, facing this variability of hydraulic loading conditions, no clear influence on suffusion susceptibility of hydraulic loading history could be drawn. Even with the same type of hydraulic loading (i.e., hydraulic-gradient controlled

[1]Associate Professor, Univ. de Nantes, Institut de Recherche en Génie Civil et Mécanique, CNRS, 58 rue Michel Ange, BP 420, F-44606 Saint-Nazaire Cedex, France; Dept. of Civil Engineering, Sultan Agung Islamic Univ., Indonesia. E-mail: abdoul.rochim@etu.univ-nantes.fr

[2]Professor, Univ. de Nantes, Institut de Recherche en Génie Civil et Mécanique, CNRS, 58 rue Michel Ange, BP 420, F-44606 Saint-Nazaire Cedex, France (corresponding author). E-mail: didier.marot@univ-nantes.fr

[3]Associate Professor, Univ. Grenoble Alpes, CNRS, 3SR, F-38000 Grenoble, France. E-mail: luc.sibille@3sr-grenoble.fr

[4]Ph.D. Student, Univ. de Nantes, Institut de Recherche en Génie Civil et Mécanique, CNRS, 58 rue Michel Ange, BP 420, F-44606 Saint-Nazaire Cedex, France; Univ. of Science and Technology—Univ. of Danang, 54 Nguyen Luong Bang St., Lien Chieu District, Da Nang City, Vietnam. E-mail: van-thao.le@etu.univ-nantes.fr

conditions) Luo et al. (2013) showed that for the tested soil, the suffusion susceptibility seems to be influenced by the increment of hydraulic gradient and by the duration of each stage. This soil appears more resistant when facing suffusion process in the "short-term experiment" (multistaged hydraulic gradient with increments ranging from 0.06 to 0.54 and with stage duration from 10 to 30 min) than in the "long-term large hydraulic head experiment" (large single-staged hydraulic gradient remained constant up to eight days).

The main objective of this paper is to investigate: (1) the suffusion susceptibility of gap and widely graded soils showing a slight variation of the initial gradation, and (2) the hydraulic loading history effects on this susceptibility. A series of downward seepage flow tests was realized under hydraulic-gradient controlled and flow-rate controlled conditions. Moreover different increments of hydraulic gradient, different flow rates, and different test durations were used. The results are discussed in terms of gradation of suffusion susceptibility. Hydraulic loading history effects on the value of critical hydraulic gradient and on the rate of erosion are studied. Finally the suffusion susceptibility is also assessed by a new energy-based method, and recommendations for suffusion tests are given.

Control Parameters for Likelihood of Suffusion

Three criteria are distinguished for suffusion to occur (Fell and Fry 2013): (1) the size of the fine soil particles must be smaller than the size of the constrictions between the coarser particles, which form the basic skeleton of the soil; (2) the volume of fine soil particles must be less than the volume of voids between coarser particles; and (3) the velocity of flow through the soil matrix must be high enough to move the loose fine soil particles through the pore. The first two criteria are associated with the fabric of granular soils, which mainly depends on the grain-size distribution. Thus to assess the potential susceptibility of a soil to suffusion, several researchers proposed methods that are only based on the study of soil gradation (U.S. Army Corps of Engineers 1953; Kenney and Lau 1985; Li and Fannin 2008; Chang and Zhang 2013 among others). However, the modification of the effective stress (Moffat and Fannin 2006; Bendahmane et al. 2008; Chang and Zhang 2011) and the relative density (Indraratna et al. 2015) can also influence the suffusion susceptibility. Finally, for a given grain-size distribution and a given value of effective stress, angularity of coarse fraction grains contributes to increase the suffusion resistance (Marot et al. 2012). The third criterion is related to the action of the fluid phase with respect to seepage loading required to detach and then to transport the fine particles. Skempton and Brogan (1994), Ke and Takahashi (2012), Indraratna et al. (2015) proposed to relate the onset of suffusion with an increase of hydraulic conductivity. Skempton and Brogan proposed to characterize the corresponding hydraulic loading by the critical hydraulic gradient. However a fraction of the detached particles can resettle or be filtered at the bulk of the porous network (Reddi et al. 2000; Bendahmane et al. 2008; Marot et al. 2009, 2011a; Nguyen et al. 2012; Luo et al. 2013). These processes can eventually induce local clogging, accompanied by variations of fluid velocity and interstitial pressure. Therefore, variations of both seepage flow and pressure gradient have to be taken into account to evaluate the hydraulic loading. By considering both of these parameters, Reddi et al. (2000) assumed that hydraulic loading can be represented by the viscous shear stress at the fluid-solid interface. They expressed this shear stress, τ, for a horizontal flow in the porous medium, and it can be reformulated for vertical flow by

$$\tau = \left(\frac{\Delta h \, \gamma_w}{\Delta z}\right) \frac{r}{2} \tag{1}$$

where Δh = drop of hydraulic head between upstream section A and downstream section B; γ_w = unit weight of water; $\Delta z = z_A - z_B$, with z_A and z_B = altitudes of sections A and B, respectively; and r = equivalent radius, representing the effects of all pores.

In the case of cohesive soils, Reddi et al. (2000) proposed to estimate the equivalent radius of pores by

$$r = \sqrt{\frac{8k\eta}{n\gamma_w}} \tag{2}$$

where n = porosity; k = hydraulic conductivity; and η = dynamic viscosity.

Consequently, the hydraulic shear stress along vertical system of capillary tubes can be expressed by

$$\tau = \left(\frac{\Delta h}{\Delta z}\right) \sqrt{\frac{2k\eta\gamma_w}{n}} \tag{3}$$

For erodibility characterization, a commonly used interpretative method for hole erosion tests (Wan and Fell 2004) consists in describing the erosion rate from the excess shear stress equation, defined by

$$\dot{m} = k_d(\tau - \tau_c) \quad \text{for } \tau \geq \tau_c \tag{4}$$

where k_d = erosion coefficient; and τ_c = critical hydraulic shear stress. The considered soil-water interface is the hole surface which is assumed to be cylindrical. Reddi et al. (2000) considered that the surface of pores is more representative for suffusion process, thus they expressed the erosion rate of soils per unit pore ($\dot{m}$) by

$$\dot{m} = \frac{m(\Delta t)}{N_p S_p \Delta t} \tag{5}$$

where m = eroded dry mass during the elapsed time Δt; N_p = number of average pores; and S_p = average pore area. Assuming an equivalent pore radius r as defined in Eq. (2), N_p and S_p can be computed respectively by

$$N_p = \frac{Sn}{\pi r^2} \tag{6}$$

$$S_p = 2\pi r L \tag{7}$$

where S = cross section area of the specimen; and L = length of the specimen.

Another way to consider variations of both seepage velocity and pressure gradient consists in expressing the power expended by the seepage flow (Marot et al. 2011b, 2016). Three assumptions are used: the fluid temperature is assumed constant, the system is considered as adiabatic, and only a steady state is considered. The energy conservation equation allows the expression of the total flow power as the summation of the power transferred from the fluid to the solid particles and the power dissipated by viscous stresses in the fluid. As the transfer between fluid and solid appears negligible in the suffusion process (Sibille et al. 2015a), the authors suggest characterizing the fluid loading from the total flow power, P_{flow}, which is expressed by

$$P_{\text{flow}} = Q \, \gamma_w \Delta h \tag{8}$$

where Q = fluid flow rate.

Marot et al. (2011b) expressed the erosion resistance index by

$$I_\alpha = -\log\left(\frac{m_{\text{dry}}}{E_{\text{flow}}}\right) \tag{9}$$
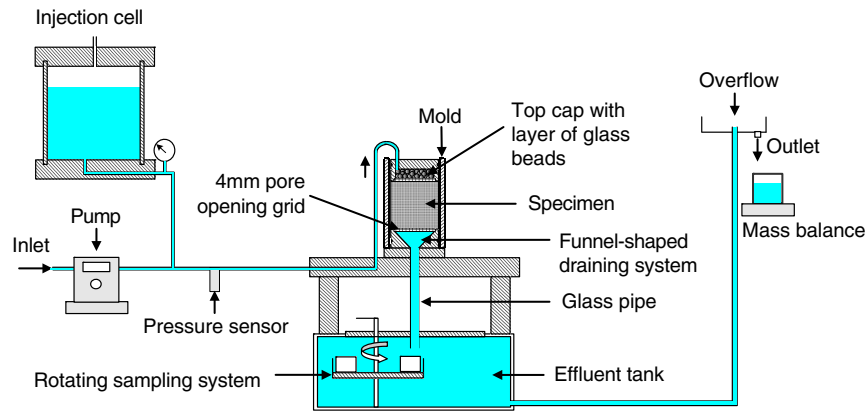
© ASCE

J. Geotech. Geoenviron. Eng.

Fig. 1. Sketch of the experimental bench

where E_{flow} = expended energy; computed by time integration of instantaneous flow power; and m_{dry} = cumulative eroded dry mass. From this energy-based method, six categories of suffusion soil sensibility are proposed: from highly resistant to highly erodible (Marot et al. 2016).

Laboratory Experiments

Main Characteristics of Testing Apparatus

The device is designed to apply downward seepage on fine soil specimens (50 mm in diameter and heights up to 100 mm) (Fig. 1). The hydraulic gradient of this seepage is controlled thanks to an injection cell equipped with pressure sensor and connected to an air/water interface cylinder. The system to generate seepage flow in flow-rate-controlled conditions comprises a gear pump connected to a pressure sensor at its outlet. The fluid passes through the top cap, which contains a layer of glass beads to diffuse the fluid uniformly on the specimen top surface. The funnel-shaped draining system is connected to an effluent tank by a glass pipe. The effluent tank is equipped with an overflow outlet (to control the downstream hydraulic head) and a rotating sampling system containing eight beakers for the sampling of eroded particles carried with the effluent. In the case of clay or silt suffusion, a multichannel optical sensor can be placed around the glass pipe (Marot et al. 2011a), and thanks to a preliminary calibration, clay or silt concentration in the effluent can be computed. At the overflow outlet of the effluent

tank, water falls in a beaker which is continuously weighed in order to determine injected flow rate. The sample is supported by a lower mesh screen and the mesh screen opening size is selected with the objective to reproduce in situ earth structures without filters, as a dike for example.

Testing Materials

Three gap-graded soils and one widely-graded soil composed of sand and gravel were tested. A laser diffraction particle-size analyzer was used to measure the grain size distribution of these soils (Fig. 2). Tests were performed with demineralized water and without deflocculation agent. Table 1 summarizes the properties of soils used in the laboratory tests. These soils were selected in order to obtain internally unstable soils. Their gradations slightly differ, mainly with respect to the fine content ranging from 20% to less than 30% (Fig. 2). According to grain size–based criteria these soils are indeed internally unstable but close to the stability limits defined by several methods currently available and detailed hereafter. For all studied soils, the uniformity coefficient C_u is around 20 [i.e., the stability boundary proposed by U.S. Army Corps of Engineers (1953)]. Minimum values of Kenney and Lau's (1985) ratio (H/F) are lower than 1 for all tested soils; thus according to this criterion, they are considered as internally unstable. As the percentage of fine particles (smaller than 0.0633 mm) is smaller than 5%,
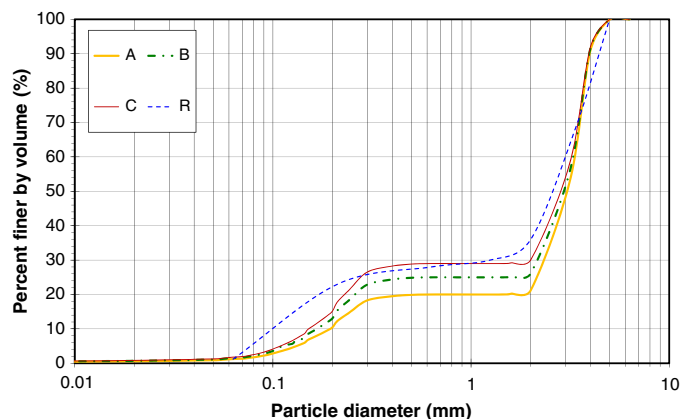

Fig. 2. Grain-size distribution of tested soils

Table 1. Properties of Tested Gradations

Properties	Tested gradations			
	A	B	C	R
P (%)	1.227	1.533	1.779	1.200
G_r	3.2	3.2	4	WG
C_u	17.06	19.52	21.07	24.46
d_{15}/d_{85}	8.761	8.741	8.724	9.653
$(H/F)_{min}$	0.038	0.035	0.033	0.165
$D\,(H/F)_{min}$ (mm)	0.400	0.400	0.400	0.212
$D_{c35}^c/d_{85,SA}^f$	3.295	3.295	3.295	2.903

Note: $D(H/F)_{min}$ = corresponding diameter with the minimum value of ratio H/F; D_{c35}^c = controlling constriction for coarser fraction from constriction size distribution by surface area technique; d_{15} and d_{85} = sieve sizes for which 15 and 85% respectively of the weighed soil is finer; $d_{85,SA}^f$ = representative size for finer fraction by surface area technique; F and H = mass percentages of the grains with a size lower than a given particle diameter d and between d and $4d$, respectively; G_r = d_{max}/d_{min} (d_{max} and d_{min} = maximal and minimal particle sizes characterizing the gap in the grading curve); WG = widely-graded soil.

and the gap ratio G_r is higher than 3, Chang and Zhang's (2013) method assessed widely-graded soil R and gap-graded soils A, B, and C as internally unstable. However, G_r value for soils A and B is slightly higher than 3, corresponding to the stability boundary proposed by Chang and Zhang. The method proposed by Indraratna et al. (2015) combines the particle size distribution and the relative density. In Table 1 values of the ratio of the controlling constriction for coarser fraction from constriction size distribution by surface area technique to the representative size for finer fraction by surface area technique ($D_{c35}^c/d_{85,SA}^f$) was computed with the highest value of specimen initial dry density discussed later in this paper. According to this method, all specimens are considered to be internally unstable.

Specimen Preparation and Testing Program

The specimen preparation phase is divided into three steps: production, installation, and then saturation of the specimen. The repeatability of the production is achieved by the following procedure. First, sand grains and gravel are mixed with a moisture content of 7.8%. To prepare these specimens, a single layer semistatic compaction technique is used, until the initial fixed dry density is reached with 50 mm specimen height. Two values of initial dry density are targeted: 90 and 97% of the optimum Proctor density. As recommended by Kenney and Lau (1985), in order to reduce preferential flow, each specimen is wrapped in a latex sleeve, then put inside a metal mold. The downstream filter is composed of a 4 mm pore opening grid. Such a pore opening allows the migration of all sand particles as in the case of earth structures without any filter. The saturation phase begins with an upward injection of carbon dioxide during 5 min to improve dissolution of gases into water; afterward, demineralized water is injected under low hydraulic gradient. The saturation process takes twelve hours, until water trickles over the top cap. With this preparation technique (Nguyen 2012), the final saturation ratio was determined by measuring density and water content, and reached 95%. Finally, the specimen is subjected to a downward flow, using demineralized water and three kinds of hydraulic loading. The choice of these hydraulic loading programs constitutes a compromise between hydraulic loadings representative of real hydraulic conditions in the field, and the possibility of characterizing the sensibility of a soil to suffusion in a couple of hours. Test duration is indeed decisive from an engineering point of view, in particular during an earth structure construction. Fig. 3 shows the time evolution of the applied
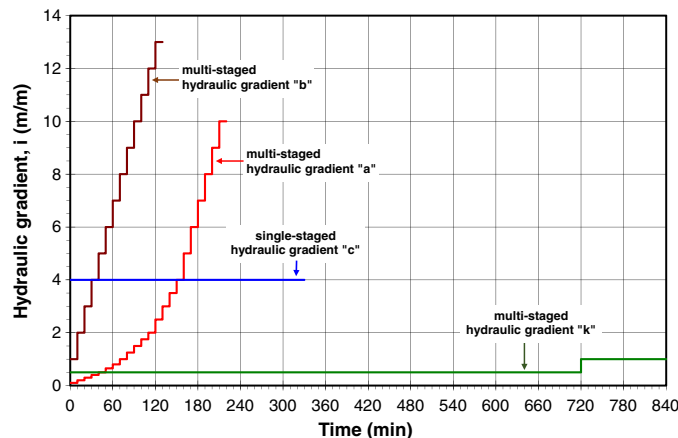
Table 2. Properties of Tested Specimens

Soil reference in paper	Specimen reference in paper	Initial dry density γ_d (kN/m³)	Applied hydraulic gradient i	Injected flow q (mL/min)	Test duration (min)
A	A-a	17.39	From 0.1 to 15	—	270
	A-a_rep	17.39	From 0.1 to 15	—	250
	A-b	17.39	From 1 to 13	—	130
	A-c	17.39	4	—	300
B	B90-a	17.39	From 0.1 to 6	—	180
	B90-c	17.39	4	—	300
	B90-k	17.39	From 0.5 to 1	—	1440
	B90-q2	17.39	—	1.641	270
	B97-a	18.74	From 0.1 to 12	—	240
	B97-b	18.74	From 1 to 9	—	90
C	C-a	18.74	From 0.1 to 9	—	210
	C-b	18.74	From 1 to 7	—	70
R	R90-a	17.39	From 0.1 to 6	—	180
	R90-b	17.39	From 1 to 8	—	80
	R97-b	18.74	From 1 to 12	—	120
	R97-q1	18.74	—	1.247	210

hydraulic gradients. Multistaged hydraulic gradients represent different increases of hydraulic loading that are more or less severe. The first multistaged hydraulic gradient condition (named a) consists of increasing the hydraulic gradient by steps of 0.1 until 2, then by steps of 0.5 between 2 and 4 and by steps of 1 beyond. For the second kind of hydraulic loading (b), the hydraulic gradient increment is directly equal to 1. For both hydraulic loadings, each stage of hydraulic gradient is kept constant for 10 min. For hydraulic loading (k) with a hydraulic gradient increment of 0.5, the duration of the hydraulic gradient stage is 12 h. Hydraulic loading (c) represents a constant hydraulic gradient of 4 in order to represent the constant hydraulic head occurring for instance in the cases of large reservoirs or canals during normal flow conditions. For this type of hydraulic loading, the hydraulic gradient is voluntarily chosen to be quite high to try to force the occurrence of suffusion (this point is based on the a priori assumption, but not always verified a posteriori, that the higher the hydraulic gradient is the more prone suffusion is to occurring). Finally with the objective to recreate the same hydraulic loading condition as used by Kenney and Lau (1985), Nguyen et al. (2012), and Ke and Takahashi (2014, 2015) in their suffusion tests, two constant flow rates are used ($q1 = 1.247$ mL $\cdot$ min^{-1} and $q2 = 1.641$ mL $\cdot$ min^{-1}, corresponding value of discharge per unit cross section 10^{-3} cm $\cdot$ s^{-1} and 1.410^{-3} cm $\cdot$ s^{-1}, respectively).

With the objective of improving readability, the first letter of each test name is related to the gradation (Fig. 2), the second letter indicates the type of hydraulic loading type, and the number details the initial relative density. Table 2 indicates the initial dry density of sixteen tested specimens, the values of applied hydraulic gradient or injected flow rate, and the duration for each test.

The repeatability of tests was verified by performing 2 tests under identical conditions: A-a and A-a_rep.

Results and Discussion

Hydraulic Behavior of Tested Specimens

The hydraulic conductivity of tested specimens are shown on Figs. 4 and 5 in the case of hydraulic loadings (a) and (b). For these types of hydraulic loadings, the hydraulic conductivity first decreases with a kinetic depending on the hydraulic loading type and also on the relative density. In the case of hydraulic loading
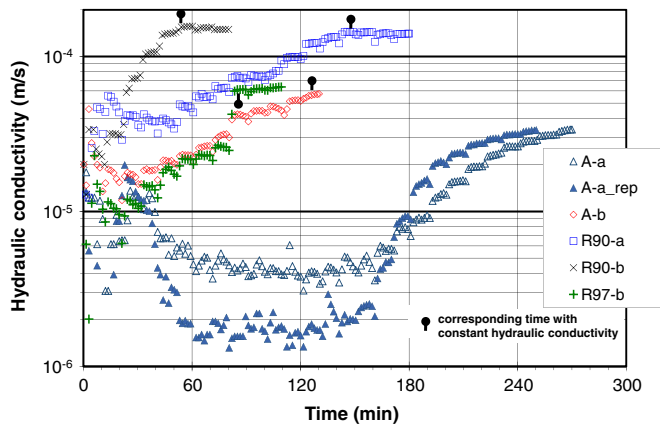

Fig. 3. Time evolution of multistaged and single-staged hydraulic gradients

Fig. 4. Time evolution of hydraulic conductivity, soils A and R, hydraulic loadings a and b

Fig. 6. Time evolution of hydraulic conductivity, tests A-c, B90-c, B90-q2, B90-k, and R97-q1

(b), the duration of this first decreasing step is from 10 min (tests C-b, B97-b, R90-b) to 20 min (tests A-b, R97-b). Whereas under hydraulic loading (a), the hydraulic conductivity decreases for a much longer time (50 min for test R90-a; 80 min for test B90-a; 120 min for tests A-a, A-a_rep, C-a and even 150 min for B97-a). For a given gradation and a given hydraulic loading, this decreasing phase is longer for a denser specimen (for example: R90-b in comparison with R97-b; and B90-a in comparison with B97-a). The second phase of hydraulic conductivity evolution is characterized by a rapid increase by a factor between 4 (test A-b) and 20 (test A-a_rep). Finally the hydraulic conductivity reaches a constant value which is pointed out by black spots on Figs. 4 and 5. The repeatability of the seepage test can be validated by comparing the initial and final values of hydraulic conductivity for tests A-a and A-a_rep, which are in good agreement. However, irregular deviation of hydraulic conductivity appears in the middle of the test. Only a few data exist in literature concerning suffusion test repeatability. Ke and Takahashi (2014) observed the same hydraulic conductivity deviation which they attributed to the difference in homogeneity among the reconstituted soil specimens. In addition the complexity of the suffusion process, highlighted by the identification of predominant processes discussed in the following section, may explain the deviation of hydraulic conductivity evolution during the suffusion development.
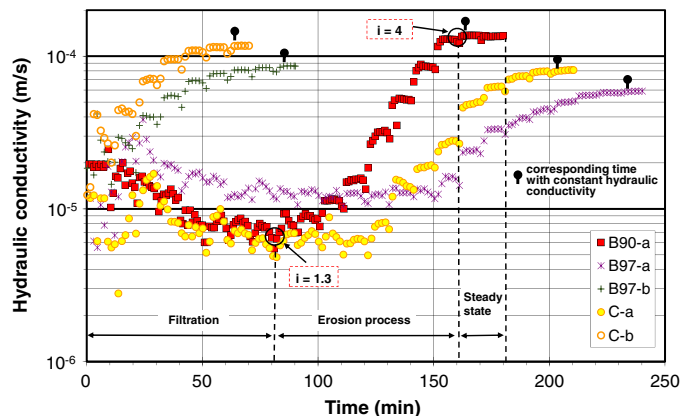
Fig. 6 shows the slow and monotonous decrease with time of the hydraulic conductivity, which is measured during single-staged hydraulic gradient tests (tests A-c, B90-c, and B90-k during the first hydraulic stage with a duration of 720 min) or under flow-rate controlled tests (tests B90-q2 and R97-q1). Thus some variations in the hydraulic loading appear necessary in order to initiate the second increasing phase of the hydraulic conductivity, even after several hours of seepage as during test B90-k (Fig. 3).

Identification of Predominant Processes

The comparison of time evolution of hydraulic conductivity with time evolution of erosion rate and measurement of post suffusion-test soil grading constitute a way to improve the understanding of the suffusion process.

Fig. 7 shows the erosion rate per unit pore area [computed by Eq. (5)] for tests B90-a, B90-c, and B90-q2. The erosion rate depends on hydraulic conductivity and porosity, which evolve in time. For the computation of porosity during time, the specimen height is assumed constant and the eroded mass measurement is taken into account.

The decrease of hydraulic conductivity is systematically accompanied by a decrease of erosion rate, which suggests that some detached particles can be filtered within the soil itself. This filtration may induce a clogging of several pores followed by a decrease of the hydraulic conductivity. Under multistaged

Fig. 5. Time evolution of hydraulic conductivity, soils B and C, hydraulic loadings a and b; identification of predominant processes during test B90-a
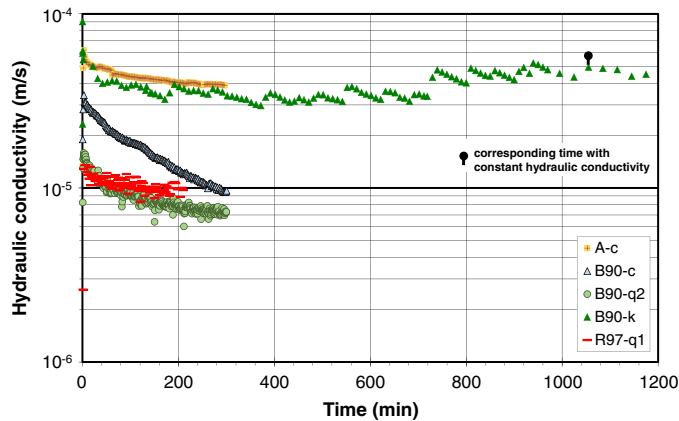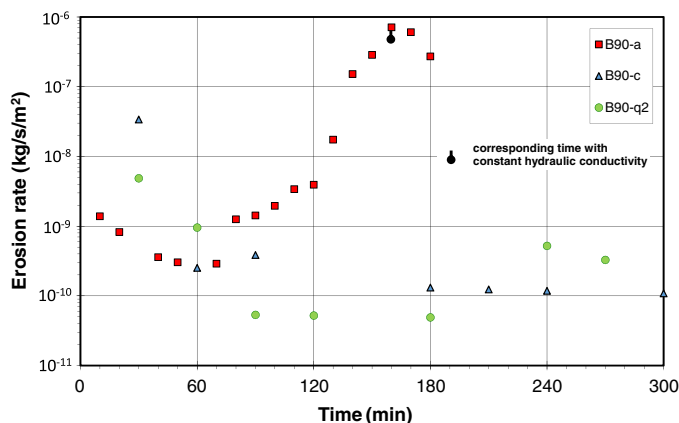

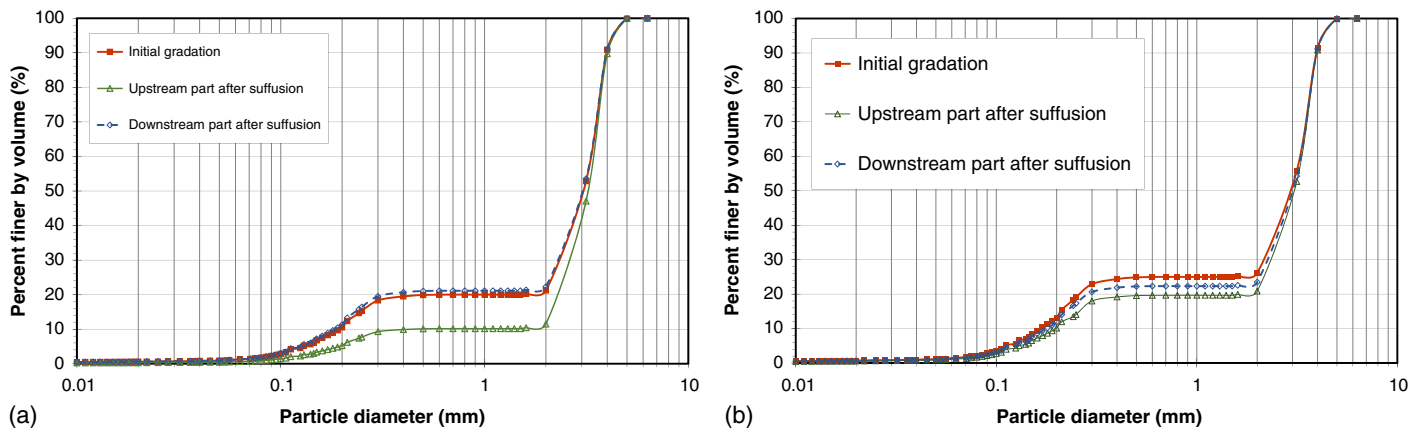**Fig. 7.** Time evolution of erosion rate, tests B90-a, B90-c, and B90-q2

Fig. 8. Initial soil gradation and gradations of upstream and downstream parts after suffusion test for (a) test A-a; (b) test B90-a

hydraulic gradient conditions, a rough increase of the erosion rate occurs simultaneously with the increase of the hydraulic conductivity. These simultaneous increases confirm that a clogging firstly restricting the water flow can be blown away by a sudden increase of the hydraulic loading. Thus the predominant process during this second phase seems to be the detachment and transport of solid particles. Finally hydraulic conductivity tends to stabilize while the erosion rate decreases. This third phase could be explained by the presence of preferential flows created by the erosion process leading to a steady state.

At the end of suffusion tests A-a and B90-a, specimens were divided in two parts named upstream and downstream parts and their grain size distributions were measured. Figs. 8(a and b) show the initial gradation and the gradation of downstream and upstream parts of soils A and B respectively. For both specimens, the loss of fine particles is higher in the upstream part. This is in agreement with the results of Ke and Takahashi (2012). The transport of detached particles from upstream to downstream parts can partly offset the loss of particles in the downstream part. Moreover, in the downstream part of specimen A, the final percentage of fines exceeds the initial percentage, which confirms the process of filtration. In the upstream part, the percentage of fine particles corresponds only to half of the initial fine percentage of specimen A, whereas it represents about 80% of the initial fine percentage in specimen B. Thus the filtration process appears to be raised by the amount of detached particles that come from the upstream part. Furthermore specimens A and B90 have the same initial density (Table 2), but different percentages of fines. For a given density, a lower fine content is accompanied with a larger amount of coarse particles and a smaller constriction size within the porous network, which facilitates the filtration process.

For a given soil, a multistaged hydraulic loading with higher increments induces a higher final value of hydraulic conductivity. Final hydraulic conductivity is higher under hydraulic loading (b) than under hydraulic loading (a) (tests A-a, A-a_rep, A-b, R90-a, and R90-b in Fig. 4 and tests B97-a, B97-b, C-a, and C-b in Fig. 5) and also higher than in the case of hydraulic loading (k) (test B90-a in Fig. 5 and test B90-k in Fig. 6). Thus an application of higher increments may limit the filtration process.

The loading by multistaged hydraulic gradient that was applied for test B90-a permits the obtainment of the three aforementioned phases, and the steady state that follows an extensive erosion is reached for $i = 4$ (Fig. 5). This same value of hydraulic gradient $i = 4$ was continuously applied during test B90-c, but this hydraulic loading leads only to the predominant process

of filtration (Fig. 6). Therefore, the history for reaching that final hydraulic gradient has a significant influence on the hydraulic behavior of specimens and on the development of suffusion.

Finally, the complex erosion phenomenon of suffusion appears as a combination of three processes: detachment, transport, and possible filtration of the finer fraction. This combination results in strong heterogeneities in soil grading and large evolutions of hydraulic conductivity and erosion rate. The development of these coupled processes depends on the grain size distribution and the density, and also on the evolution of hydraulic loading, which in turns is influenced by the suffusion development.

Characterization of Suffusion Onset

Fig. 9 shows the flow velocity versus the hydraulic gradient for tests on soil B. With the objective to determine with accuracy the onset of suffusion, the relative evolution of hydraulic conductivity is computed, and the onset of suffusion is systematically defined by the first relative increase of 10%. First, under single-staged hydraulic gradient conditions and under flow-rate controlled conditions (tests B90-c and B90-q2 respectively, on Fig. 9), the determination of the suffusion onset with such an approach is not possible. For tests realized under multistaged hydraulic gradient conditions, the values of the critical hydraulic gradient are indicated in Table 3. The critical hydraulic gradient appears higher with hydraulic loading (b) than with hydraulic loading (a) for soils
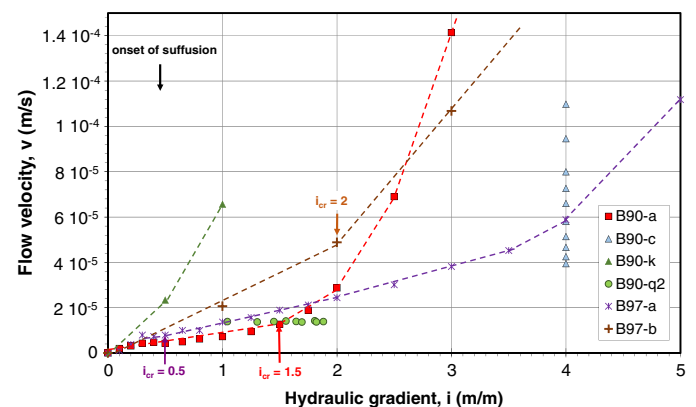

Fig. 9. Flow velocity versus hydraulic gradient, critical hydraulic gradient, soil B

Table 3. Critical Hydraulic Gradient, Multistaged Hydraulic Gradient Conditions

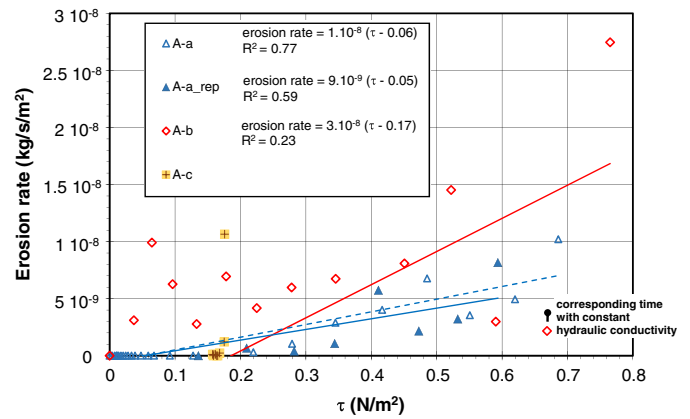| Tested specimens	Critical hydraulic gradient i_c	
	Hydraulic loading (a)	Hydraulic loading (b)
A	3.5–3.9	4.5
B90	1.5	—
B97	0.5	2
C	2.5	2.5
R90	0.6	1.8
R97	—	3.4

A, B97, and R90. In consequence, for a given soil the critical hydraulic gradient seems to depend on the history of hydraulic loading. This influence of hydraulic loading history was also observed by Luo et al. (2013) who compared the results obtained with two test durations. They notably concluded that a long-term large hydraulic head reduces the hydraulic gradient needed for major suffusion development.

For both hydraulic loadings, the comparison of the critical hydraulic gradient obtained for tested soils shows that soil A requires a larger hydraulic gradient to initiate the suffusion process. The initial gradation of this soil has a lower fine content (20%) in comparison with soil B (initial fine content of 25%), and soils C and R (initial fine content about 29%). These results are in good agreement with the test results presented by Ke and Takahashi (2012) on cohesionless soils with three different initial fine contents from 16.7 to 25%.

Characterization of Suffusion Development

As for other internal erosion processes, a first interpretative method for suffusion tests could consist in representing the erosion rate as a function of the hydraulic shear stress. As for erosion rate computation [Eq. (5)], the computation of hydraulic shear stress [Eq. (3)] takes into account the time evolutions of hydraulic conductivity and porosity. Value of porosity corresponds to an average value that characterizes the whole specimen, without distinction between upstream and downstream parts. However, thanks to the hydraulic conductivity evolutions, Eq. (3) takes partially into account the development of specimen heterogeneities during the course of the experiment.

Fig. 10 shows the erosion rate versus the hydraulic shear stress for tests on soil A. Thanks to the aforementioned identification of suffusion onset, based on hydraulic conductivity increase, it is possible to define the initiation of the suffusion development phase. The end of this phase is assumed to be reached at the stabilization of the hydraulic conductivity. Now by considering only tests realized under hydraulic loadings (a) and (b), a linear approximation representing Eq. (4) is computed. Fig. 10 shows the corresponding equation with values of k_d, τ_c, and the correlation coefficient R^2 for tests A-a, A-a_rep, and A-b. The erosion rate versus the hydraulic shear stress is basically close for tests A-a and A-a_rep which might imply the good repeatability of the suffusion test. Table 4 details the values of erosion coefficient and correlation coefficient for tested specimens under multistaged hydraulic gradient conditions. First, the weak values of correlation coefficient (between 0.01 for test B97-a, and 0.77 for test A-a) highlight the difficulty of describing the erosion rate from this approach. These low values of correlation coefficient cannot be attributed to the imprecision of the determination of erosion rate and hydraulic shear stress, which can be valued at $\pm 3 \times 10^{-11}$ kg $\cdot$ s^{-1} $\cdot$ m^{-2} and ± 0.02 Pa respectively. Moreover, the erosion coefficient values obtained with hydraulic

Fig. 10. Erosion rate versus hydraulic shear stress, soil A

Table 4. Erosion Coefficient and Correlation Coefficient, Multistaged Hydraulic Gradient Conditions

Tested specimens	Hydraulic loading (a)		Hydraulic loading (b)	
	Erosion coefficient k_d (s/m)	Correlation coefficient R^2	Erosion coefficient k_d (s/m)	Correlation coefficient R^2
A	10^{-8}–9×10^{-9}	0.77–0.59	3×10^{-8}	0.23
B90	10^{-6}	0.54	—	—
B97	4×10^{-7}	0.01	7×10^{-7}	0.05
C	6×10^{-7}	0.08	10^{-6}	0.04
R90	8×10^{-7}	0.15	2×10^{-6}	0.06
R97	—	—	2×10^{-7}	0.02

loading (b) are systematically higher (with a factor between 1.4 and 3.3) than in the case of hydraulic loading (a). Thus the characterization of suffusion susceptibility based on this interpretative method depends on the history of hydraulic loading. Moreover, in the case of flow-rate controlled condition tests or single-staged hydraulic gradient tests (A-c on Fig. 10) and even under hydraulic loading (k), a single value of hydraulic shear stress can be associated with a large range of erosion rates. Consequently, it is not possible to describe with accuracy the erosion rate by such interpretative methods.

With the objective to take into account the history of hydraulic loading, the energy expended by the seepage flow E_{flow} is determined by the time integration of total flow power, P_{flow} [computed by Eq. (8)] for the test duration. Figs. 11–14 show the cumulative loss of dry mass, m_{dry}, versus the cumulative expended energy for all kinds of hydraulic loading.

For characterizing the erosion susceptibility, the erosion resistance index is computed at the end of the test, which is determined by the stabilization of the hydraulic conductivity, pointed out by black spots on Figs. 11–14. If the test is stopped before the stabilization of the hydraulic conductivity, the erosion resistance index is computed with the last realized measurements. Table 5 indicates the values of erosion resistance index for all realized tests.

When the stabilization of the hydraulic conductivity is reached, the corresponding value of the erosion resistance index, written in bold in Table 5, can be determined with accuracy for the different hydraulic loadings. The erosion resistance index I_α is between 3.40 and 3.64 for tests B97 (i.e., this soil is moderately erodible according to the suffusion susceptibility classification proposed by Marot et al. 2016), between 3.03 and 3.09 for tests C (moderately
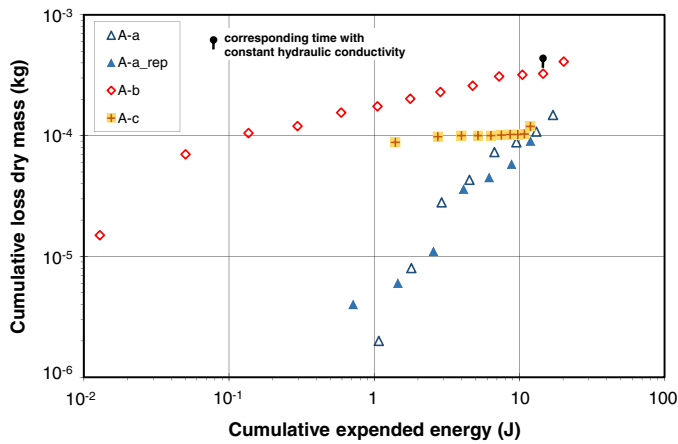
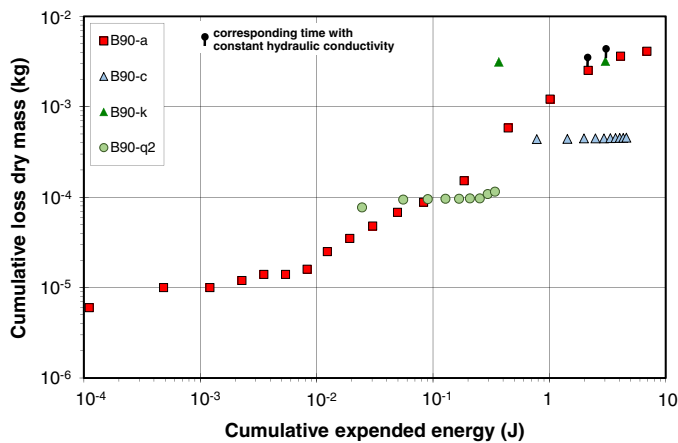**Fig. 11.** Cumulative loss of dry mass versus cumulative expended energy, soil A

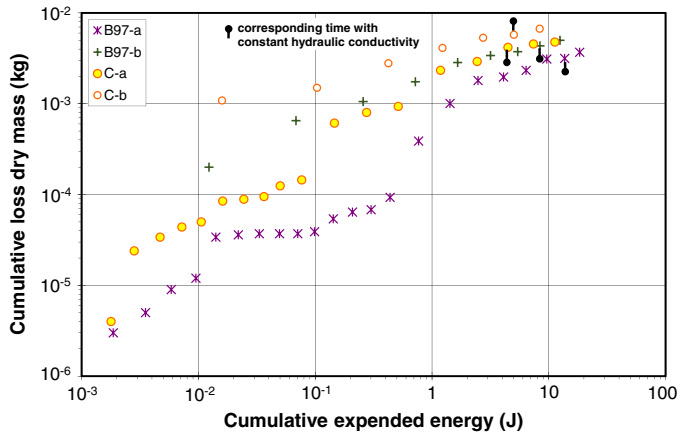**Fig. 12.** Cumulative loss of dry mass versus cumulative expended energy, tests B90-a, B90-c, B90-k, and B90-q2

Fig. 13. Cumulative loss of dry mass versus cumulative expended energy, tests B97-a, B97-b, C-a, and C-b
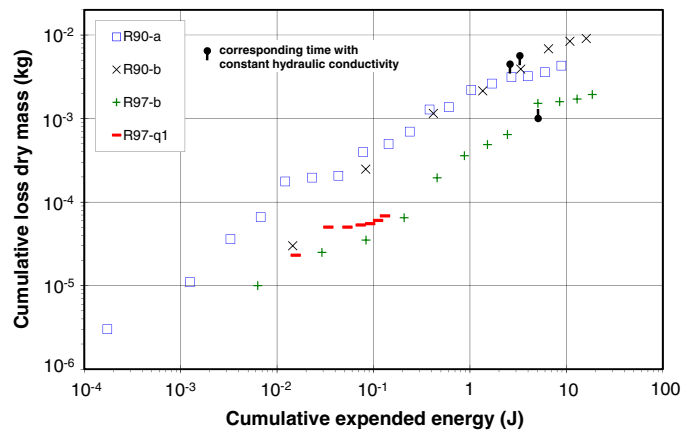
Fig. 14. Cumulative loss of dry mass versus cumulative expended energy, soil R

Table 5. Erosion Resistance Index

| Tested specimens | Erosion resistance index I_α | | | | |
	Hydraulic loading (a)	Hydraulic loading (b)	Hydraulic loading (c)	Hydraulic loading (k)	Hydraulic loading ($q1-q2$)
A	5.06–5.12	**4.65**	5.00	—	—
B90	**2.93**	—	3.25	**2.98**	3.47
B97	**3.64**	**3.40**	—	—	—
C	**3.03**	**3.09**	—	—	—
R90	**2.94**	**2.94**	—	—	—
R97	—	**3.52**	—	—	3.29

Note: Values in bold indicate corresponding erosion resistance index when the stabilization of the hydraulic conductivity is reached.

resistance index and thus an overestimation of the soil resistance. This shows the necessity to perform suffusion tests by increasing the applied hydraulic gradient in order to be able to follow the development of all possible processes and to continue the test to the point at which hydraulic conductivity becomes constant.

The comparison of erosion resistance indexes obtained for tests B90 and B97 on one hand, and for tests R90 and R97 on the other hand, permits highlighting the positive influence of density on the soil resistance face suffusion process (both soils are erodible with initial dry density of 17.39 kN/m³ and moderately erodible with initial dry density of 18.74 kN/m³). These results are in good agreement with the results obtained by Indraratna et al. (2015) who showed that the increase of relative density permits transformation of unstable specimens into stable ones. By considering tests characterized by a constant final hydraulic conductivity, for soils B, C ,and R the erosion resistance index is between 2.93 and 3.64, whereas it reaches 4.65 for test A-b (corresponding suffusion susceptibility classification: moderately resistant). Thus soil A, which contains less fine particles (initial fine content: 20%), appears more resistant than soils B (initial fine content: 25%), C (initial fine content about 29%), and R (initial fine content about 29%). Thanks to the aforementioned interpretation of posttest grading, it is possible to conclude that the higher resistance of soil A is mainly due to the increase in filtration in the specimen's downstream part.

Finally even if tested soils were unstable according to grain size distribution–based criteria, the suffusion susceptibility classification for tested specimens is between erodible (B90-a, R90-a, and R90-b) and moderately resistant (A).

erodible), between 2.93 and 2.98 for tests B90 (erodible), and equal to 2.94 for tests R90 (erodible). On the other hand, if the test is stopped before the stabilization of the hydraulic conductivity, interpretation can lead to a higher value of the erosion

Recommendations for Testing

According to the aforementioned results, several recommendations can be drawn to perform suffusion tests:

1. Even if grain size distribution–based criteria lead to internally unstable states for all studied soils, a gradation of soil suffusion susceptibility can be obtained according to slight variations of initial soil grading and density; thus suffusion tests have to be performed;

2. Suffusion is the result of the combination of three processes: detachment, transport, and filtration, which in particular depend on the history of hydraulic loading; with the objective of following the development of all possible combinations, tests must be realized by increasing the applied hydraulic gradient, and it should be carried on until the stabilization of the hydraulic conductivity; and

3. The hydraulic loading on one hand, and the induced erosion on the other hand, must be independently characterized; thus the energy dissipated by the water seepage, E_{flow}, and the cumulative loss of dry mass are computed respectively; finally at the end of each test, which corresponds to the invariability of the hydraulic conductivity, the erosion sensibility classification can be evaluated by the value of the erosion resistance index.

Conclusion

The characterization of suffusion susceptibility is an important issue for contributing to the safety assessment of hydraulic earth structures. Tests realized under different hydraulic loading histories highlight the complexity of suffusion, which can be understood as the process by which the finest soil particles are detached and transported within the porous soil network. Detached particles can be filtered out with an increasing rate depending on initial gradation, density, and evolution of hydraulic loading.

According to the type of hydraulic loading, the predominant process can be either filtration or erosion. Thus even if a transport of particles is geometrically possible, the action of hydraulic loading must be studied.

The analysis of the suffusion onset can be carried out by determining the critical hydraulic gradient. However, the realized study shows that the type of hydraulic loading can substantially modify the value of the critical hydraulic gradient at which suffusion occurs. For other erosion processes, the interpretative method can consist in describing the erosion rate by using the excess shear stress equation. In the case of suffusion, the influence of the hydraulic loading history on the erosion coefficient value and the weak values of correlation coefficient show that such an approach does not permit to determine a unique suffusion susceptibility characterization.

A new interpretative method is proposed, linking the cumulative eroded dry mass to the energy dissipated by the fluid flow. This method is efficient for determining the suffusion susceptibility for cohesionless material. This study also shows the necessity of performing suffusion tests by increasing the applied hydraulic gradient and continuing tests until hydraulic conductivity becomes constant.

Acknowledgments

References

Bendahmane, F., Marot, D., and Alexis, A. (2008). "Experimental parametric study of suffusion and backward erosion." *J. Geotech. Geoenviron. Eng.*, 10.1061/(ASCE)1090-0241(2008)134:1(57), 57–67.

Chang, D. S., and Zhang, L. M. (2011). "A stress-controlled erosion apparatus for studying internal erosion in soils." *J. ASTM Geotech. Test.*, 34(6), 579–589.

Chang, D. S., and Zhang, L. M. (2013). "Extended internal stability criteria for soils under seepage." *Soils Found.*, 53(4), 569–583.

Fell, R., and Fry, J. J. (2007). *Internal erosion of dams and their foundations*, Taylor & Francis, London.

Fell, R., and Fry, J. J. (2013). *Erosion in geomechanics applied to dams and levees*, S. Bonelli Ed., ISTE—Wiley, London, 1–99.

Fry, J. J., Vogel, A., Royet, P., and Courivaud, J. R. (2012). "Dam failures by erosion: Lessons from ERINOH data bases." *Proc., 6th Int. Conf. on Scour and Erosion*, Paris, 273–280.

Indraratna, B., Israr, J., and Rujikiatkamjorn, C. (2015). "Geometrical method for evaluating the internal instability of granular filters based on constriction size distribution." *J. Geotech. Geoenviron. Eng.*, 10.1061/(ASCE)GT.1943-5606.0001343, 04015045.

Ke, L., and Takahashi, A. (2012). "Strength reduction of cohesionless soil due to internal erosion induced by one dimensional upward seepage flow." *Soils Found.*, 52(4), 698–711.

Ke, L., and Takahashi, A. (2014). "Triaxial erosion test for evaluation of mechanical consequences of internal erosion." *Geotech. Test. J.*, 37(2), 20130049.

Ke, L., and Takahashi, A. (2015). "Drained monotonic responses of suffusional cohesionless soils." *J. Geotech. Geoenviron. Eng.*, 10.1061/(ASCE)GT.1943-5606.0001327, 04015033.

Kenney, T. C., and Lau, D. (1985). "Internal stability of granular filters." *Can. Geotech. J.*, 22(2), 215–225.

Li, M., and Fannin, J. (2008). "Comparison of two criteria for internal stability of granular soil." *Can. Geotech. J.*, 45(9), 1303–1309.

Luo, Y. L., Qiao, L., Liu, X. X., Zhan, M. L., and Sheng, J. C. (2013). "Hydro-mechanical experiments on suffusion under long-term large hydraulic heads." *Nat. Hazards*, 65(3), 1361–1377.

Marot, D., Bendahmane, F., and Konrad, J. M. (2011a). "Multi-channel optical sensor to quantify particle stability under seepage flow." *Can. Geotech. J.*, 48(12), 1772–1787.

Marot, D., Bendahmane, F., and Nguyen, H. H. (2012). "Influence of angularity of coarse fraction grains on internal erosion process." *La Houille Blanche, Int. Water J.*, 6(6), 47–53.

Marot, D., Bendahmane, F., Rosquoët, F., and Alexis, A. (2009). "Internal flow effects on isotropic confined sand-clay mixtures." *Soil Sediment Contam., Int. J.*, 18(3), 294–306.

Marot, D., Regazzoni, P. L., and Wahl, T. (2011b). "Energy based method for providing soil surface erodibility rankings." *J. Geotech. Geoenviron. Eng.*, 10.1061/(ASCE)GT.1943-5606.0000538, 1290–1293.

Marot, D., Rochim, A., Nguyen, H. H., Bendahmane, F., and Sibille, L. (2016). "Assessing the susceptibility of gap graded soils to internal erosion: proposition of a new experimental methodology." *Nat. Hazards*, 83(1), 365–388.

Moffat, R., and Fannin, J. (2006). "A large permeameter for study of internal stability in cohesionless soils." *J. ASTM Geotech. Test.*, 29(4), 273–279.

Nguyen, H. H. (2012). "Caractérisation de mécanismes d'érosion interne: Confrontation d'érodimètres et d'approches." Ph.D. thesis, Université de Nantes, France.

Nguyen, H. H., Marot, D., and Bendahmane, F. (2012). "Erodibility characterisation for suffusion process in cohesive soil by two types of hydraulic loading." *La Houille Blanche, Int. Water J.*, 6(6), 54–60.

Reddi, L. N., Lee, I., and Bonala, M. V. S. (2000). "Comparison of internal and surface erosion using flow pump test on a sand-kaolinite mixture." *J. ASTM Geotech. Test.*, 23(1), 116–122.

Sibille, L., Lominé, F., Poullain, P., Sail, Y., and Marot, D. (2015a). "Internal erosion in granular media: Direct numerical simulations and energy interpretation." *Hydrol. Processes*, 29(9), 2149–2163.

Sibille, L., Marot, D., and Sail, Y. (2015b). "A description of internal erosion by suffusion and induced settlements on cohesionless granular matter." *Acta Geotechnica*, 10(6), 735–748.

Skempton, A. W., and Brogan, J. M. (1994). "Experiments on piping in sandy gravels." *Géotechnique*, 44(3), 440–460.

U.S. Army Corps of Engineers. (1953). "Filter experiments and design criteria." *Technical Memorandum No. 3-360*, Waterways Experiment Station, Vicksburg, VA.

Wan, C. F., and Fell, R. (2004). "Investigation of rate of erosion of soils in embankment dams." *J. Geotech. Geoenviron. Eng.*, 10.1061/(ASCE) 1090-0241(2004)130:4(373), 373–380.

Wan, C. F., and Fell, R. (2008). "Assessing the potential of internal instability and suffusion in embankment dams and their foundations." *J. Geotech. Geoenviron. Eng.*, 10.1061/(ASCE)1090-0241(2008)134: 3(401), 401–407.